THE STATUS OF CLAY MINERAL STRUCTURES

by

S. W. BAILEY

Department of Geology
University of Wisconsin, Madison, Wisconsin

ABSTRACT

THE basic outlines of most of the hydrous layer silicate structures were determined during the 1930's. Present escalating interest in obtaining additional detail is indicated by (a) publication of over twenty structural refinements (2-D or 3-D) during 1954–64, (b) publication of at least nine structures in 1965 or early 1966, and (c) personal communication that at least fifteen additional refinements are in progress. Points of especial interest in these recent studies follow.

1. Octahedral cation order is common, but tetrahedral cation order is confirmed in only three cases. Because ordering of Si, Al does not significantly affect the statistical tests for centrosymmetry, centrosymmetric space groups that do not permit order should be avoided during refinement.

2. Oversize tetrahedral sheets articulate with smaller octahedral sheets by tetrahedral rotation and, for dioctahedral species, by tetrahedral tilting around vacant octahedra. The latter mechanism influences the type and regularity of layer sequences. Undersize tetrahedral sheets articulate with larger octahedral sheets by tilting plus octahedral contraction or by inversion of some tetrahedra.

3. The amount and direction of tetrahedral rotation and tilt, length of T—O, M—O, and O—O bonds, sheet thicknesses, and relation of cell dimensions to composition can now be predicted with some confidence.

4. Variation in layer stacking (polytypism) is common. In some cases the stabilities of different polytypes can be explained by the relative amounts of repulsion and attraction between the ions in the structures. The stabilities can be correlated with the energy available in the environment of crystallization.

INTRODUCTION

THE basic outlines of most of the hydrous layer silicates were determined during the 1930's, principally by John Gruner and Sterling Hendricks in extension of the Pauling structures. During the past ten years there has been renewed interest in obtaining additional detail on these structures using modern structural methods and repeated refinement cycles with electronic computing machines. During 1954–64 at least twenty-two two-dimensional and three-dimensional refinements of hydrous layer silicates were published, exclusive of those with inverted tetrahedra or cylindrical lattices. In addition, at least nine refinements will be published in 1965 or early 1966, with fifteen

https://doi.org/10.1346/CCMN.1966.0140101 Published online by Cambridge University Press

structure determinations known to be still in progress (Fig. 1). Included among the in-press (*) and in-progress investigations are the following:

7 Å types	9½ Å types	10 Å types	14 Å types
kaolinite	pyrophyllite	polylithionite	vermiculite*
nacrite	talc	muscovite-3T	cookeite
3-layer Al-serpentine	minnesotaite	seybertite	gonyerite
6-layer Al-serpentine		biotite	dioctahedral chlorite*
cronstedtite		Li fluophlogopite	Ib ($\beta = 90°$) chlorite*
bementite			
lizardite*			Ib ($\beta = 97°$) chlorite

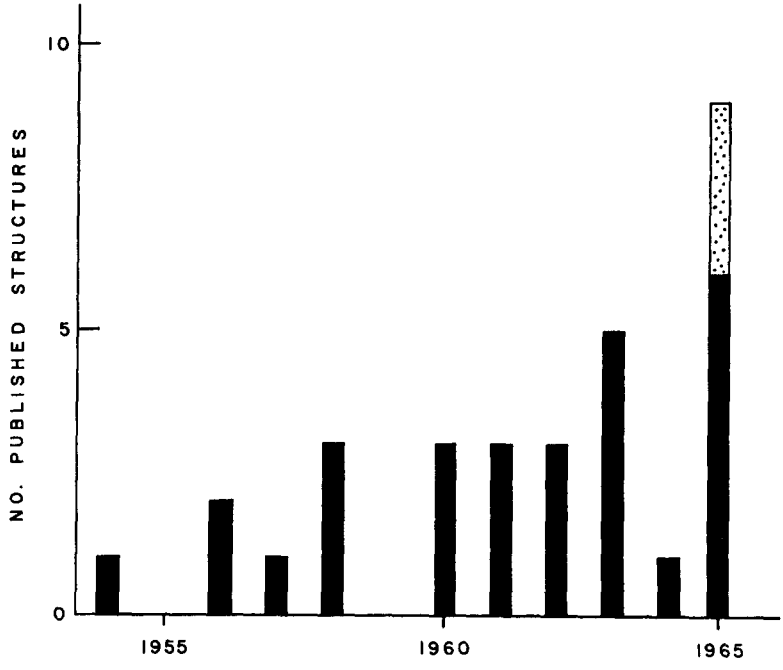


FIG. 1. Histogram of published two-dimensional and three-dimensional refinements of clay mineral structures, exclusive of those with inverted tetrahedra or cylindrical lattices. Stippled area for 1965 includes articles in press at time of writing.

https://doi.org/10.1346/CCMN.1966.0140101 Published online by Cambridge University Press

It is noteworthy that in addition to the increasing number of structure determinations of clays being done in recent years the number of X-ray reflections being used and the number of refinement cycles are also increasing. We are justified in placing correspondingly more faith in the reliability of the results. An understanding or an explanation of the structural features of clay minerals, however, is not necessarily the same as a knowledge of the atomic positions within the structures. It is gratifying, therefore, both to see a number of recent papers devoted primarily to the crystal chemistry of layer silicates and, within individual structure determination papers, to see more emphasis being placed on the interpretation of results and comparison with other structures.

The present paper will summarize some of the recent literature regarding the interpretation of selected structural features of layer silicates. It will also make use of the results of the structural symposium at the 13th Clay Conference and of unpublished research to illustrate certain of these features and to point out some unsolved problems.

Previously unpublished research on nacrite, dioctahedral chlorite, I*b* chlorite, cookeite, and vermiculite cited in this paper was supported in part by grant 1176–A2 from the Petroleum Research Fund, administered by the American Chemical Society, and in part by grants GP–412, GP–2197, and GP–3748 from the National Science Foundation.

OCTAHEDRAL CATION ORDERING

Veitch and Radoslovich (1963) have proposed on theoretical grounds that octahedral cations of different size and valence will tend to adopt an ordered distribution. Cations with high valence either occupy two sites, leaving the third site vacant or nearly so, or else they occupy one site with the other two essentially filled with larger mono and divalent cations. This general tendency is confirmed in most, but not all, of the recent detailed structural studies (Table 1).

The vacant site has been found to be ordered in all dioctahedral species so far investigated. In fact, heating studies at 600°C on pyrophyllite, paragonite, hydrous mica, and montmorillonite by Lindqvist (1962) indicate that when two cations are distributed randomly over three octahedral sites $d(060)$ increases to such an extent that the mineral would not be recognizable as dioctahedral. Slightly more than one-half of the trioctahedral species investigated show some degree of octahedral cation order. Corundophyllite is listed as disordered only because of the evidence of equal electron density peaks cited by the author to show that there is no preferential segregation of the 0.42 atoms of Fe + Cr. In reality all chlorites must at least have ordering between sheets to assure a positive charge on the brucite sheet. Some evidence that there is ordering of Mg and Al between sheets in corundophyllite is given by smaller M—O distances in the brucite sheet. In most of the disordered cases listed in Table 1*a* cation order is either impossible because of the

https://doi.org/10.1346/CCMN.1966.0140101 Published online by Cambridge University Press

TABLE 1.—OCTAHEDRAL CATION DISTRIBUTIONS

(a) Within one octahedral sheet

Dioctahedral species	M_1	M_2	Trioctahedral species	M_1	M_2
kaolinite	□	Al_2	cronstedtite—1T	$(Fe_2^{2+}Fe^{3+})$	disordered*
dickite	□	Al_2	cronstedtite—$2H_1$	$(Fe_2^{2+}Fe^{3+})$	disordered*
nacrite	□	Al_2	cronstedtite—3T	$(Fe_2^{2+}Fe^{3+})$	disordered
pyrophyllite	□	Al_2	amesite—$2H_2$	(Mg_2Al)	disordered*
celadonite—1M	$Mg_{0.1}$	$(Fe_{1.4}^{3+}Mg_{0.6})$	phlogopite—1M	Mg_3	
muscovite—$2M_1$	□	Al_2	ferriphlogopite—1M	Mg_3	
paragonite—$2M_1$	□	Al_2	ferri-annite—1M	Fe_3	
margarite—$2M_1$	□	Al_2	xanthophyllite—1M	$(Mg_{1/2}Al_{1/2})$	Mg_2

(b) Within two octahedral sheets

Species	M_1	M_2	M_3	
cookeite (I*a*)	□	Al	Al	pyrophyllite sheet
	Li	Al	Al	"brucite" sheet
vermiculite (I*a*)	Mg	Mg	Mg	talc sheet
	$Mg_{0.4}$	□	□	interlayer
prochlorite (II*b*-2)	$(Mg_{3/4}Fe_{1/4}^{2+})$	$Fe_{0.9}^{3+}$	Mg	talc sheet
	$Mg_{3/4}$	$(Al_{3/4}Fe_{1/4}^{3+})$	$(Al_{3/4}Fe_{1/4}^{3+})$	brucite sheet
kammererite (I*a*-4)	Mg	Mg	Mg	talc sheet
	$(Cr_{0.7}Al_{0.2}Mg_{0.1})$	Mg	Mg	brucite sheet
ripidolite (I*b*-90°)	$(Fe_{2.0}^{2+}Mg_{0.8}Al_{0.2})$	disordered*		talc sheet
	$(Fe_{1.4}^{2+}Mg_{0.5}Al_{1.1})$	disordered*		brucite sheet
corundophyllite (II*b*-4)	$(Mg_{4.9}Al_{0.8}Fe_{0.2}^{3+}Cr_{0.2})$	"disordered"		

* Space group does not permit ordering within sheet.

In order to preserve space, references to the individual structures are not given here but may be found by consulting the other listed references. The trioctahedral 7Å polytype symbols are from Bailey (in preparation).

composition involved or is not permitted by the space group chosen for refinement purposes. The difficulty in choosing the true space group for layer silicates is discussed in a following section.

OCTAHEDRAL SHEET CONFIGURATION

Dioctahedral

Figure 2 illustrates an idealized dioctahedral sheet with six Al^{3+} cations arranged in a hexagon around each vacant octahedral site. Given this hexagonal arrangement, the attractive and repulsive forces present within the sheet will distort the sheet in the following ways.

https://doi.org/10.1346/CCMN.1966.0140101 Published online by Cambridge University Press

(1) Adjacent Al^{3+} cations will repel one another and move farther apart. Coordinating anions on the shared octahedral edges will tend to partially shield the Al cations by moving towards one another in the directions shown by arrows in Fig. 2. Because each anion is pulled in only one direction,

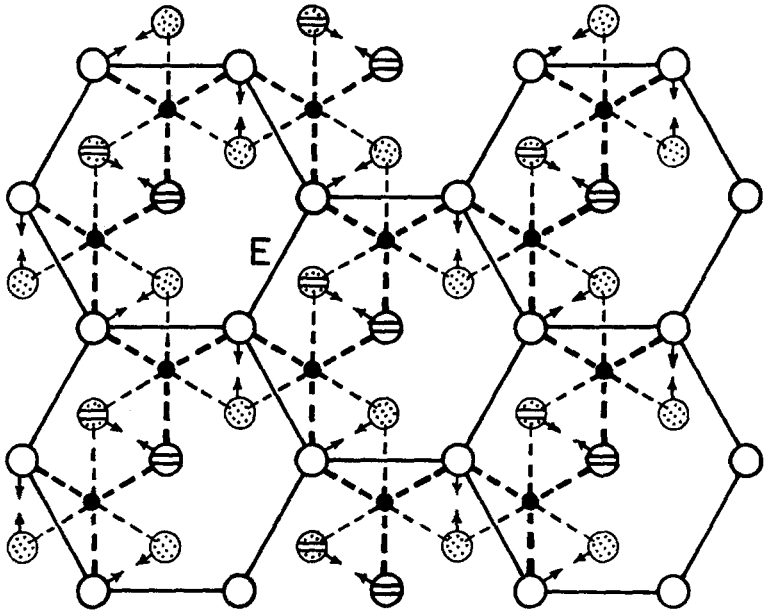


FIG. 2. Idealized dioctahedral sheet of a 2:1 layer. Thin stippled circles are anions in lower plane, thick open circles are anions in upper plane, and small solid circles are octahedral Al ions. Anions on shared octahedral edges move in directions indicated by arrows to minimize cation repulsion. Modified from Takéuchi (1965).

extreme shortening of shared edges results. Observed O—O and OH—OH shared edge lengths are in the range from 2.3 to 2.5 Å in contrast to values from 2.7 to 2.9 Å for unshared edges (Table 2).

(2) Because of the shortening of the shared octahedral edges the entire octahedral sheet is thinned along the sheet normal and is expanded along X and Y within the sheet. Typical sheet thicknesses are 2.04 to 2.10 Å for Al compositions (Table 3).

(3) The lateral edges of the triads around the vacant site are expanded due to the outward movement of these anions as a result of shared edge shortening. These edges, illustrated by E in Fig. 2, characteristically measure 3.2 to 3.4 Å in dioctahedral Al-clays. Figure 3 illustrates the size of the vacant site relative to the occupied sites in the case of nacrite.

https://doi.org/10.1346/CCMN.1966.0140101 Published online by Cambridge University Press

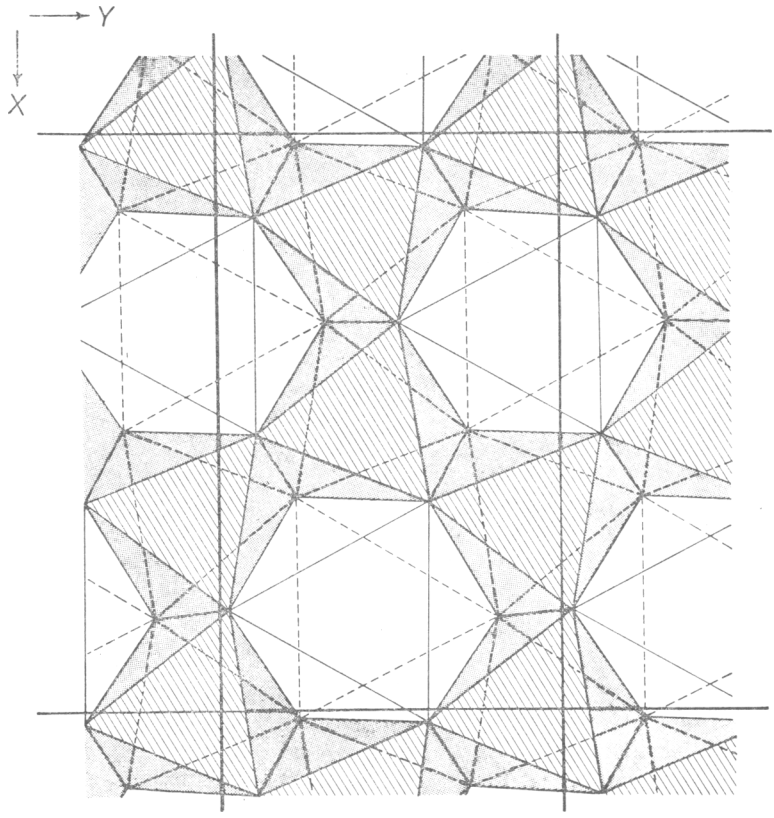


FIG. 3. Relative sizes of occupied and vacant octahedral sites in nacrite (Threadgold, 1963).

(4) The direction of movement of anions on shared edges is such as to rotate the upper and lower octahedral triads in opposite directions. This same movement distorts the hexagonal pattern of anions by an alternate clockwise and anticlockwise twisting of two-thirds of the hexagon edges. The resultant distorted octahedral network, illustrated for the case of margarite in Fig. 4, contains four twisted short edges and two long edges within each hexagon. The effect of this distortion on the tetrahedral sheet and on polytypism will be discussed in following sections.

Trioctahedral

For trioctahedral clays lateral cation repulsion is less than for the dioctahedral case because of the smaller charge per cation. Each anion is now pulled in three directions along three shared edges, instead of along one edge

https://doi.org/10.1346/CCMN.1966.0140101 Published online by Cambridge University Press

TABLE 2.—AVERAGE OCTAHEDRAL EDGE LENGTHS

(a) Dioctahedral

	Shared (Å)	Unshared		
		Lateral (Å)	Diagonal (Å)	Vacancy (Å)
kaolinite	2.50	2.85	2.77	3.22
dickite	2.36	2.78	2.84	3.43
nacrite	2.36	2.78	2.83	3.42
muscovite	2.42	2.80	2.88	3.43
paragonite	2.42	2.78	2.87	3.40
margarite	2.42	2.77	2.86	3.37
celadonite	2.99	2.99	3.02	3.05

(b) Trioctahedral

	Shared (Å)	Unshared (Å)
amesite	2.69	3.07
cronstedtite	2.85	3.17
phlogopite	2.81	3.05
xanthophyllite	2.75	3.00
ferri-annite	2.81	3.14
ferriphlogopite	2.85	3.10
prochlorite	2.77	3.10
	2.62	3.11
corundophyllite	2.72	3.09
	2.61	3.09
kammererite	2.79	3.08
	2.70	3.08
ripidolite	2.82	3.11
	2.67	3.11
vermiculite	2.80	3.09
	2.96	3.09

as in Fig. 2. The anion cannot move directly along any shared edge as a result, only inward along the sheet normal, which is the resultant of the forces. For this reason trioctahedral sheets are nearly as thin as dioctahedral sheets (Table 3). In the case of chlorites, which have two octahedral sheets, the brucite sheet in the interlayer tends to be thinner than that in the 2:1 talc portion because of the presence in the former of sufficient R^{3+} cations to maintain its positive charge. This leads to greater lateral cation repulsion in the brucite sheet, hence expansion laterally but thinning along the sheet normal.

Because of the limitations on the direction of movement of octahedral anions, shared octahedral edges for trioctahedral clays are only slightly shorter than unshared edges. Observed average values for shared edges range

https://doi.org/10.1346/CCMN.1966.0140101 Published online by Cambridge University Press

TABLE 3—OCTAHEDRAL SHEET THICKNESSES

(a) One octahedral sheet

Dioctahedral (Å)		Trioctahedral (Å)	
kaolinite	2.10	amesite	2.02
dickite	2.04	cronstedtite	2.19
muscovite	2.09	phlogopite	2.19
paragonite	2.09	xanthophyllite	2.15
margarite	2.07	ferri-annite	2.15
celadonite	2.46	ferriphlogopite	2.22

(b) Two octahedral sheets

	2:1 Unit (Å)	Interlayer (Å)
prochlorite (II*b*)	2.11	1.90
corundophyllite (II*b*)	2.05	1.91
kammererite (I*a*)	2.15	2.03
ripidolite (I*b*)	2.18	1.98
dioctahedral chlorite (II*b*)	2.05	2.15
vermiculite (I*a*)	2.17	2.34

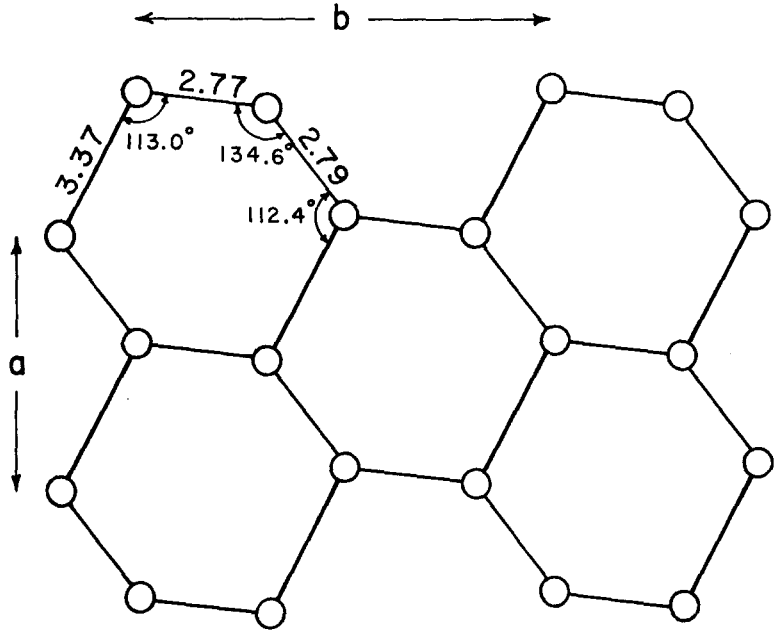


FIG. 4. Distorted oxygen network at the octahedral–tetrahedral junction in dioctahedral margarite (Takéuchi, 1965).

https://doi.org/10.1346/CCMN.1966.0140101 Published online by Cambridge University Press

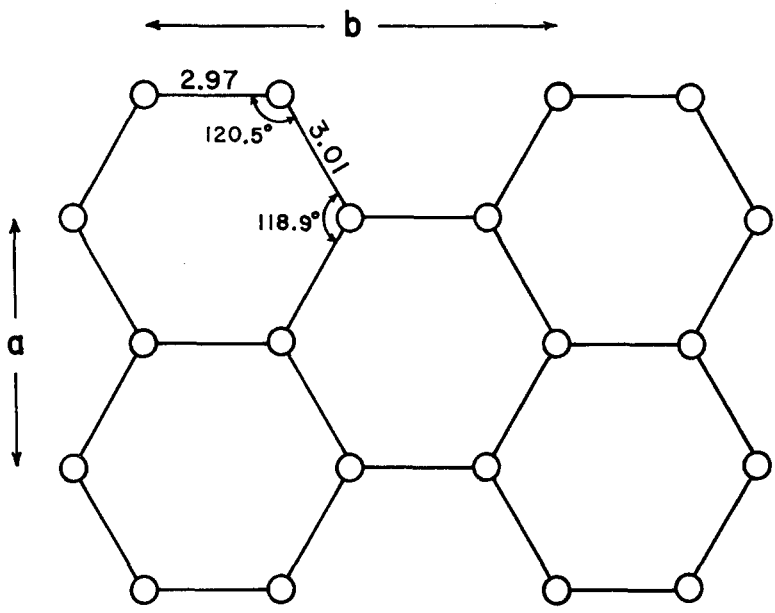


FIG. 5. Distorted oxygen network in trioctahedral xanthophyllite (Takéuchi, 1965).

from 2.6 to 2.9 Å and for unshared edges from 3.0 to 3.2 Å (Table 2). Aside from variations due to cation ordering the octahedra are more regular in size than their dioctahedral counterparts and do not have twisted edges. Figure 5 illustrates the octahedral network of oxygen hexagons for the case of xanthophyllite.

ARTICULATION OF OCTAHEDRAL AND TETRAHEDRAL SHEETS

Importance of Octahedral Sheet

One of the recent developments in the crystal chemistry of silicates has been the increased emphasis placed on the importance of the octahedral network in determining the nature of the resultant structure. In particular, the size of the octahedra and their linkage pattern are believed to have a controlling influence on the pattern of linkage of SiO_4 groups and their geometry of articulation with the octahedral network. This change in viewpoint has spread to layer silicates also, so that in many recent papers the octahedral sheet is considered to be either the dominant structural element or at least equal in status to the tetrahedral sheet, in contrast to its former secondary role. The importance of the octahedral sheet in the resultant

https://doi.org/10.1346/CCMN.1966.0140101 Published online by Cambridge University Press

structure is verified when we consider the influence of its size and configuration on the tetrahedral sheet.

Although we can measure the relative sizes of octahedral and tetrahedral sheets as joined together in a layer structure, it is difficult to assess their sizes in the free state. Figure 6 suggests, however, that the b parameter for an unconstrained tetrahedral sheet would be approximately 9.04 Å for composition Si_4Al_0 and 9.50 Å for composition Si_2Al_2. These values can be compared with equivalent parameters of 8.65 Å measured for gibbsite and bayerite [$Al(OH)_3$] and 9.36 Å measured for brucite [$Mg(OH)_2$]. This comparison, which is only a crude approximation to the actual situation, suggests that the tetrahedral sheet will be larger than the octahedral sheet for all dioctahedral Al-rich species and for trioctahedral species with appreciable tetrahedral substitution. Tetrahedral sheets with little or no substitution will be smaller than octahedral sheets containing primarily Mg and Fe.

Tetrahedral Rotation

The lateral dimensions of the tetrahedral sheet can be readily reduced to fit with a smaller octahedral sheet by the mechanism of tetrahedral rotation. An alternate clockwise and anticlockwise twist of the tetrahedra about the sheet normal will reduce the lateral dimensions according to the expression

$$\cos \alpha = b(\text{obs})/b(\text{tetr})$$

where α is the angle of rotation, b(obs) is the observed or resultant b parameter, and b(tetr) is the initial b parameter of the unconstrained sheet. The amount of lateral reduction obtained varies from 1.5% for $\alpha = 10°$ to 6.0% for $\alpha = 20°$ and a maximum of 13.4% for $\alpha = 30°$. Because the tetrahedra rotate in opposite directions the symmetry of the network changes from hexagonal to approximately ditrigonal.

The amount of tetrahedral rotation to be expected for a given layer silicate can be predicted, provided b(tetr) can be estimated. An estimate of b(tetr) can be obtained either by assuming regular tetrahedra and a particular variation of the T—O bond length with tetrahedral composition or by assuming a particular variation of the basal oxygen—oxygen distance with composition. The writer prefers the latter method because of the sensitivity of the calculated angle of rotation to deviation from tetrahedral regularity.

It can be shown for a regular hexagonal network that

$$b(\text{tetr}) = (A + B)\sqrt{3} \quad (\text{for } \alpha = 0°)$$

where A and B refer to the average of the basal oxygen—oxygen distances in tetrahedra of different sizes. Figure 6 shows that there is a fairly regular variation with tetrahedral composition of b(tetr) values obtained in this manner from basal oxygen—oxygen distances that have been measured in refined structures. Table 4 compares the observed α values for these structures with those calculated by means of the indicated line of best fit in Fig. 6 and the known tetrahedral compositions.

https://doi.org/10.1346/CCMN.1966.0140101 Published online by Cambridge University Press

TABLE 4.—TETRAHEDRAL ROTATION ANGLES

Dioctahedral	Obs.*	Calc.	Trioctahedral	Obs.*	Calc.
kaolinite	11.3°	(9.4°)	amesite	12.4°	13.9°
dickite	7.3	8.5	xanthophyllite	23.0	23.0
nacrite	~7.9	9.8	phlogopite	5.9	(8.8)
muscovite	12.8	(14.5)	prochlorite	9.4	10.3
paragonite	15.9	(16.1)	corundophyllite	7.7	7.9
margarite	21.0	20.8	kammererite	6.2	4.5
celadonite	13.2	9.0	ripidolite	5.0	(1.7)
pyrophyllite	~10.5	9.4	vermiculite	5.7	5.6
			dioct. chlorite	7.6	(9.3)

* Obtained by calculation of the O_b–O_b–O_b angles from the published atomic coordinates and cell dimensions.

Observed values for nacrite and pyrophyllite obtained during preliminary refinement cycle.

Parentheses indicate specimens for which no chemical analysis available.

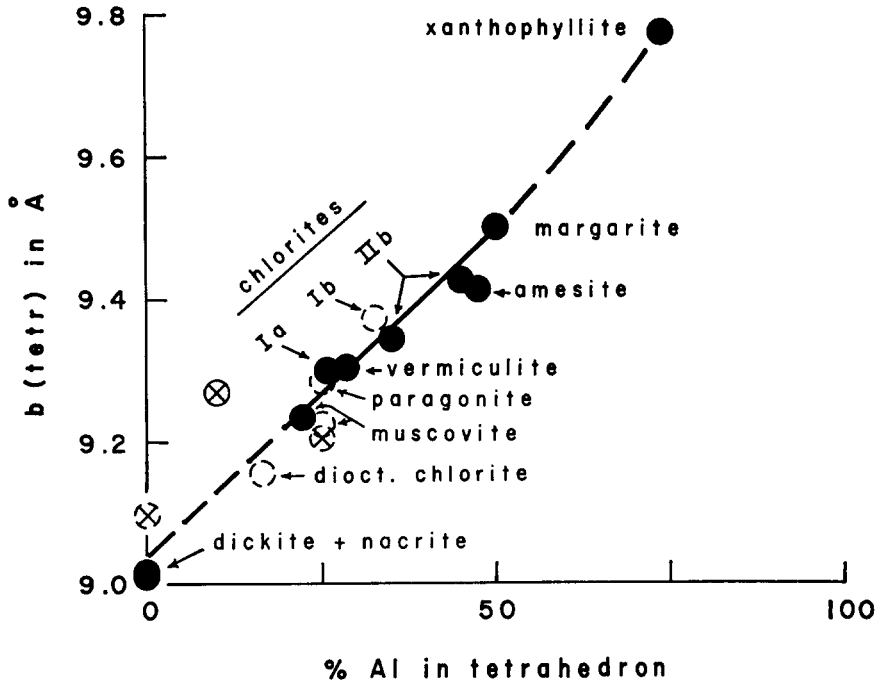


FIG. 6. Variation of lateral dimension of an unconstrained tetrahedral sheet as a function of Si, Al content. Dashed circles indicate no chemical analysis available. Crossed circles represent electron diffraction studies on kaolinite, celadonite, and phlogopite-biotite (left to right).

https://doi.org/10.1346/CCMN.1966.0140101 Published online by Cambridge University Press

Direction of Rotation

The direction of tetrahedral rotation appears to be influenced by different factors in different mineral groups. In mica structures the basal oxygens in both tetrahedral sheets move toward the positions of the nearest octahedral cations in the same layer. This is observed in all nine mica structures that have been refined to date. No other factor is involved because of the restriction in layer stacking inherent in a mica as a result of the "anchoring" effect of the interlayer cation. In 14 Å structures the additional influence of long hydrogen bonds to the basal oxygens from adjacent interlayer OH and H_2O surfaces must be considered. In five chlorite and two vermiculite structures that have been refined, the basal oxygens always move toward the nearest interlayer anion. This direction may be toward or away from the octahedral cations in the 2:1 talc portion of the structure or in the interlayer, so that the interlayer bond is the dominant factor. Figure 7 summarizes the observed relationships for the four 14 Å layer types that are theoretically possible.

In 7 Å structures the influence of the octahedral cation in the next layer, here considered to be below the basal oxygen surface, is the dominant factor for the trioctahedral species that have been examined. The basal oxygens are closer to these lower octahedral cations than to those above. Thus it is observed that the basal oxygens rotate toward the octahedral cation in the layer below in amesite-$2H_2$, in cronstedtite-1T, and in two 6-layer forms of amesite and cronstedtite. This direction is always away from the nearest hydroxyl below and may be either to or away from the octahedral cation above. In cronstedtite-3T the tetrahedral cations are superimposed over the lower octahedral cations so that rotation of the basal oxygens toward the latter is physically impossible. In this situation the oxygens rotate toward the direction of the nearest hydroxyl and upper octahedral cation, which are also vertically superposed.

In the three dioctahedral kaolins, on the other hand, the rotation direction is always toward the superposed lower hydroxyl and upper octahedral cation. This direction is away from the octahedral cation in the layer below in the case of nacrite. For kaolinite and dickite, rotation toward the lower octahedral cation is physically impossible for the same reason as in cronstedtite-3T.

Structural Adjustments

For trioctahedral layer silicates the octahedra tend to be regular and the lateral triad edges similar in size (Fig. 5). Even in cases involving cation order the deviation of individual unshared edge lengths from the mean is usually less than $\pm$ 2% and is not known to exceed $\pm$ 5%, in contrast to the usual deviation of $\pm$ 10% for dioctahedral species. An oversize tetrahedral sheet, which is the common case because of extensive tetrahedral substitution in most trioctahedral clays, can fit onto this regular octahedral

https://doi.org/10.1346/CCMN.1966.0140101 Published online by Cambridge University Press

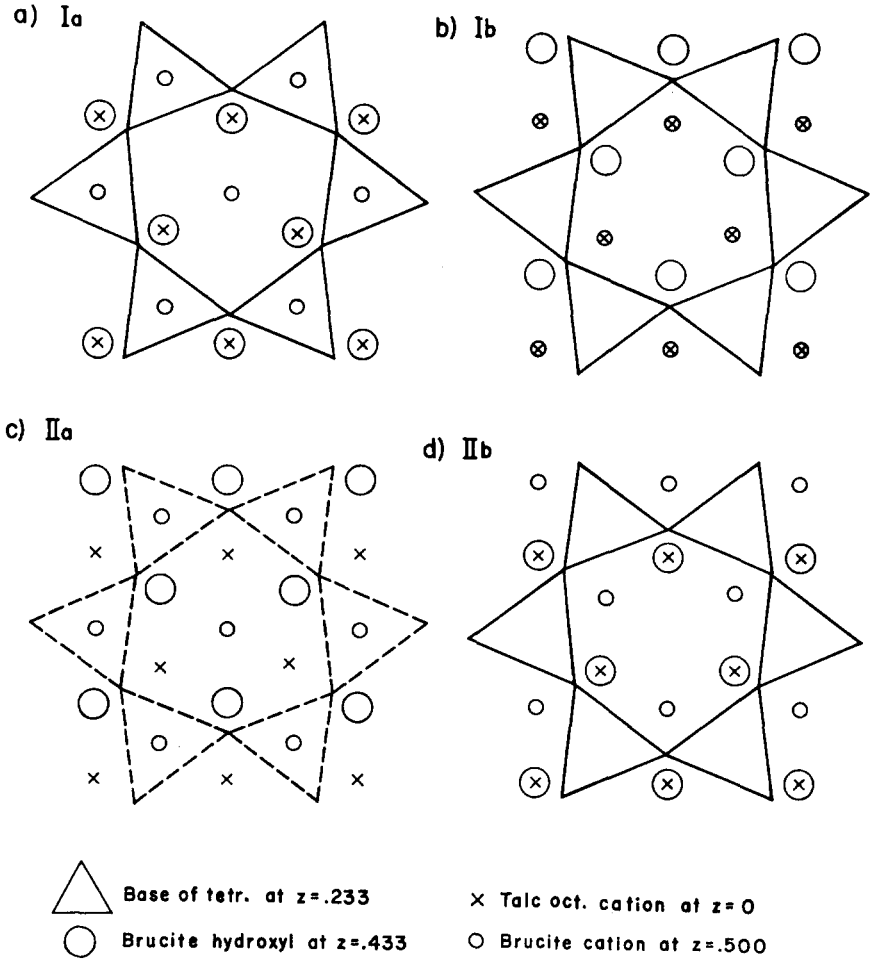


FIG. 7. Structural features, including tetrahedral twist, of four chlorite layer types in [001] projection. Expected distortion of IIa layer, so far unknown in nature, is by analogy with other layer types (Shirozu and Bailey, 1965).

surface with a minimum amount of stress by the simple mechanism of uniform lateral compression as a result of tetrahedral rotation. There is little, if any, perturbation of the basal oxygen surface. Because such lateral compression tends to bring the tetrahedral cations closer together, it is likely that the octahedral sheet will stretch to articulate with the tetrahedral sheet and to keep cation repulsion at a minimum.

For Al-rich dioctahedral species an additional structural adjustment must be made. Even though it has been indicated that an Al-rich octahedral sheet

https://doi.org/10.1346/CCMN.1966.0140101 Published online by Cambridge University Press

has smaller average lateral dimensions than a tetrahedral sheet of any composition, Fig. 4 shows that each hexagon within the octahedral sheet is distorted so that there are four short, twisted edges and two elongate edges. Each oxygen in the hexagon is also the apex of a tetrahedron. Tetrahedra linked to the short edges can adjust by tetrahedral rotation, as previously described. The two elongate hexagon edges, however, are larger than the corresponding apical oxygen–oxygen distances in a tetrahedral sheet. This adjustment can be made only by tilting the tetrahedra so that the apices

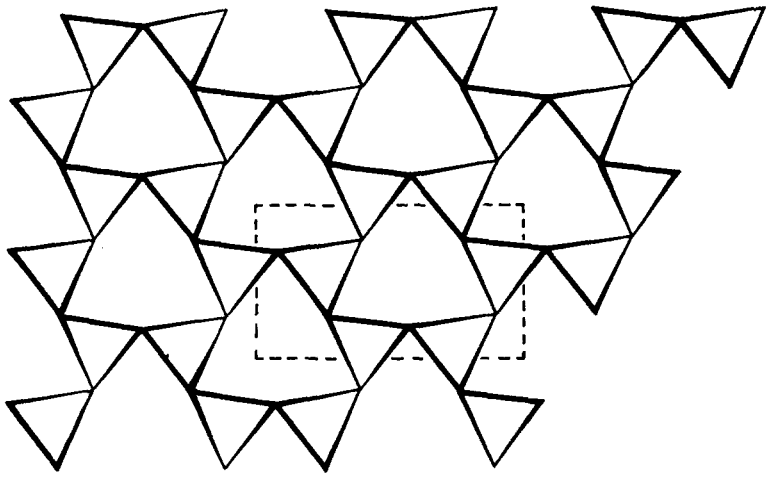


FIG. 8. Corrugation of basal oxygen surface in dioctahedral margarite. Heavy lines represent elevated tetrahedral edges (apices down) within upper tetrahedral sheet of 2:1 layer. Corrugations alternate parallel to [110] and [1$\bar{1}$0] in successive layers (Takéuchi, 1965).

of adjacent tetrahedra point away from one another on each elongate octahedral edge. Because of the tilting the tetrahedral basal oxygens become noncoplanar. The bridging oxygen between two tilted tetrahedra with apices down is depressed 0.1 to 0.2 Å below the other two basal oxygens to form a corrugation or welt that, in all dioctahedral structures refined to date, transects the structure normal to the direction of the elongate vacant site edge and parallel to the direction of sheet shift within the 2:1 unit. Figure 8 illustrates the corrugation for the case of margarite.

In some dioctahedral micas the corrugation of the basal oxygen surface has the effect of displacing the interlayer cation from the center of its cavity toward the vacant site and thereby causing a deviation of the observed β angle from the ideal. Because of tetrahedral rotation there are only six nearest neighbors around the interlayer cation instead of twelve. Radoslovich (1963) has presented evidence that in dioctahedral K-micas the K atom is too

https://doi.org/10.1346/CCMN.1966.0140101 Published online by Cambridge University Press

large for its 6-coordinated hole after tetrahedral rotation. This has the result of reducing the amount of tetrahedral rotation, of propping apart the basal oxygen surfaces, and of stretching the octahedral sheet laterally. For a smaller interlayer cation and the same composition otherwise one would expect a larger tetrahedral rotation, less interlayer separation, and a smaller b value. These are all observed in the structure of paragonite relative to muscovite by Burnham and Radoslovich (1965). Burns and White (1963) have also shown that the b value decreases as K is leached from muscovite. Donnay, Donnay, and Takeda (1964) have calculated nomograms that show the effect of K—O bond length, as well as T—O and M—O, on the resultant b repeat.

In cases where the octahedral sheet is larger than the tetrahedral sheet in all lateral directions, the tendency should be for tetrahedral tilting along all hexagon edges. If there are no additional structural constraints this leads to layer curvature with the octahedral sheet on the convex side and the tetrahedral basal oxygens on the concave side, as in the curled tubes of chrysotile asbestos. In antigorite a similar curling tendency is interrupted periodically by inversion of the tetrahedra, creating a superstructure along the X direction. Different patterns of tetrahedral inversion to relieve misfit tetrahedral and octahedral sheets are found in the minerals sepiolite, palygorskite, stilpnomelane, pyrosmalite, and zeophyllite.

In addition to the structural adjustments due to tetrahedral rotation, tilt, and inversion, both the octahedral and tetrahedral sheets can adjust their thicknesses considerably to achieve articulation. The variations found in octahedral thicknesses for different minerals (Table 3) are about two times as large as the variations in tetrahedral thicknesses (Table 5). The effect of adjustment in octahedral thickness can be illustrated by the structure of a dioctahedral chlorite in which the octahedral sheet in the 2:1 portion is dioctahedral (Al_2) and the interlayer sheet is trioctahedral ($Mg_{2\cdot3}Al_{0\cdot7}$). One might at first consider such a structure implausible because of expected lateral misfit. In fact, the structure determination (Eggleton and Bailey, 1966) shows that the misfit is accommodated by thinning the dioctahedral sheet slightly to 2.05 Å and thickening the trioctahedral sheet considerably to 2.15 Å so that the lateral edges of both octahedral sheets are identical. The brucite sheet thickness of 2.15 Å is to be compared with more customary values of 1.90 to 2.03 Å for similar composition interlayers (Table 3). It is likely that similar variations in thickness are needed to fit together the sheets in talc and saponite, where the curling tendency should be similar to chrysotile but is constrained by the presence of two tetrahedral sheets. A nomogram by Donnay *et al.* (1964) shows the effect of octahedral sheet thickness on the resultant b value.

TETRAHEDRAL CATION ORDER

In contrast to the many confirmed cases of octahedral cation order, only three examples of tetrahedral cation order are known for layer silicates. These are a kammererite, a prochlorite, and a vermiculite. Surprisingly,

https://doi.org/10.1346/CCMN.1966.0140101 Published online by Cambridge University Press

TABLE 5.—TETRAHEDRAL SHEET THICKNESS

Dioctahedral (Å)		Trioctahedral (Å)	
kaolinite	2.17	amesite	2.29
dickite	2.30	cronstedtite	2.41
muscovite	2.24	phlogopite	2.17
paragonite	2.24	ferriphlogopite	2.28
margarite	2.33	ferri-annite	2.32
celadonite	2.18	xanthophyllite	2.34
dioct. chlorite	2.30	prochlorite	2.28
		corundophyllite	2.29
		kammererite	2.26
		ripidolite	2.25
		vermiculite	2.25

none of the nine mica structures refined to date show tetrahedral cation order.

In attempting to analyze the reason for the lack of ordering it is noted in nine out of the twenty-two refined structures in which tetrahedral substitution occurs that either the space group used or the method of refinement used did not permit detection of tetrahedral cation order. This is true, for example, if there is only one independent tetrahedron in the space group, as in $C2/m$—the ideal space group for the 1M mica polytype. It is also true of any refinement that makes use of only the strong $k = 3n$ reflections and ignores the weaker, often streaked, $k \neq 3n$ reflections. In some of the other structural refinements it is doubtful that the accuracy attained was sufficient to detect ordering.

It is unusual for a layer silicate space group to have more than two independent tetrahedra. This means that for most clays the maximum ordering possible for an overall composition of Si_3Al is $Si_{1/2}Al_{1/2}$ in one tetrahedron and Si_1Al_0 in the other tetrahedron. Let us assume that it is of scientific interest to detect ordering for cases at half this level, i.e. with compositions for the two tetrahedra of $Si_{5/8}Al_{3/8}$ and $Si_{7/8}Al_{1/8}$. According to the standard bond lengths expected for Si and Al in tetrahedral coordination (Smith and Bailey, 1963) the T—O distance should be 1.676 Å for the Al-rich tetrahedron and 1.638 Å for the Si-rich tetrahedron.

In order to prove statistically whether an observed difference of 0.038 Å between two *mean* bond lengths is real (greater than three standard deviation units), the standard deviation of an *individual* T—O bond length must be less than 0.018 Å. Thus, if $\sigma(T—O) \leqq 0.018$ Å the standard error of the mean of four T—O values is $\sigma_n = \sigma(T—O)/\sqrt{n} \leqq 0.009$ Å and the standard deviation unit for comparing the two mean values is

$$\sigma = [\sigma_n^2(T_1) + \sigma_n^2(T_2)]^{1/2} \leqq 0.013 \text{ Å}$$

Values of $\sigma(T—O)$ for layer silicates in the literature range from 0.003 Å to

https://doi.org/10.1346/CCMN.1966.0140101 Published online by Cambridge University Press

0.040 Å. The accuracy of about one-third of the refined structures is insufficient to detect Si, Al ordering at the indicated level by this test.

Determination of the true space group of a layer silicate is made difficult by several problems. The observed diffraction aspect usually is not completely definitive, although it narrows the choice to two or three possible space groups. The choice is usually between a centrosymmetric and a non-centrosymmetric space group, for example $C2/c$ or Cc. The statistical tests for a center of symmetry may or may not work for a layer silicate. The strong $k = 3n$ reflections exhibit hypersymmetry because of the many atoms that repeat at intervals of $b/3$. Figure 9 shows that use of $k \neq 3n$ reflections in the $N(z)$ test may or may not reveal the true symmetry. Similarly inconsistent results were obtained using the $P(y)$, variance and Wilson ratio tests for centrosymmetry.

A further problem is that it is quite feasible that the symmetry of the distribution of tetrahedral Si and Al atoms could be lower than that of the rest of the structure and, furthermore, could not be detected by present methods. The diffraction aspect and statistical tests (when working) refer to the major structural features, such as the stacking of anion planes and the distribution of strongly scattering elements. The ordering of Si and Al over the tetrahedral positions constitutes only a minor perturbation of these major features, even considering the distortions that occur in the coordination around the larger Al and the smaller Si. Figure 9*b* shows that ordering to an acentric space group within an otherwise centrosymmetric layer structure has practically no effect on the $N(z)$ test in a calculated hypothetical case. Proof that such cases can occur in nature is given by the structure determination of a prochlorite by Steinfink (1958, 1961). The ideal space group for this particular layer sequence and for most of the atoms in the structure is $C2/m$, which allows only one independent tetrahedron. Refinement in $C2/m$ would necessarily classify the tetrahedral cations as disordered. The structure was refined as $C2$, however, and the two independent tetrahedra were shown to be significantly different in size. In fact, the indicated compositions of $Si_{0.3}Al_{0.7}$ for T_1 and $Si_{0.9}Al_{0.1}$ for T_2 represent the greatest degree of order so far found in a layer silicate. Crystallographers would do well to heed this example and to consider seriously the possibility of using a reduced symmetry if the indicated space group does not permit ordering.

Nevertheless, we now have several examples, such as muscovite-$2M_1$ and paragonite-$2M_1$, where the accuracy of the structural refinement is unquestioned and the space group permits at least partial tetrahedral order, but where no order is observed. Because muscovite and paragonite occur in the the same rock with other minerals that are completely ordered, for example microcline and albite, we must conclude that tetrahedral ordering is more difficult for a layer silicate. This may be a result of a slightly different crystallization and cooling history and of the lower degree of polymerization and covalent nature of a layer relative to a framework structure, hence related also to ease of tetrahedral substitution. It may also be of importance that

https://doi.org/10.1346/CCMN.1966.0140101 Published online by Cambridge University Press

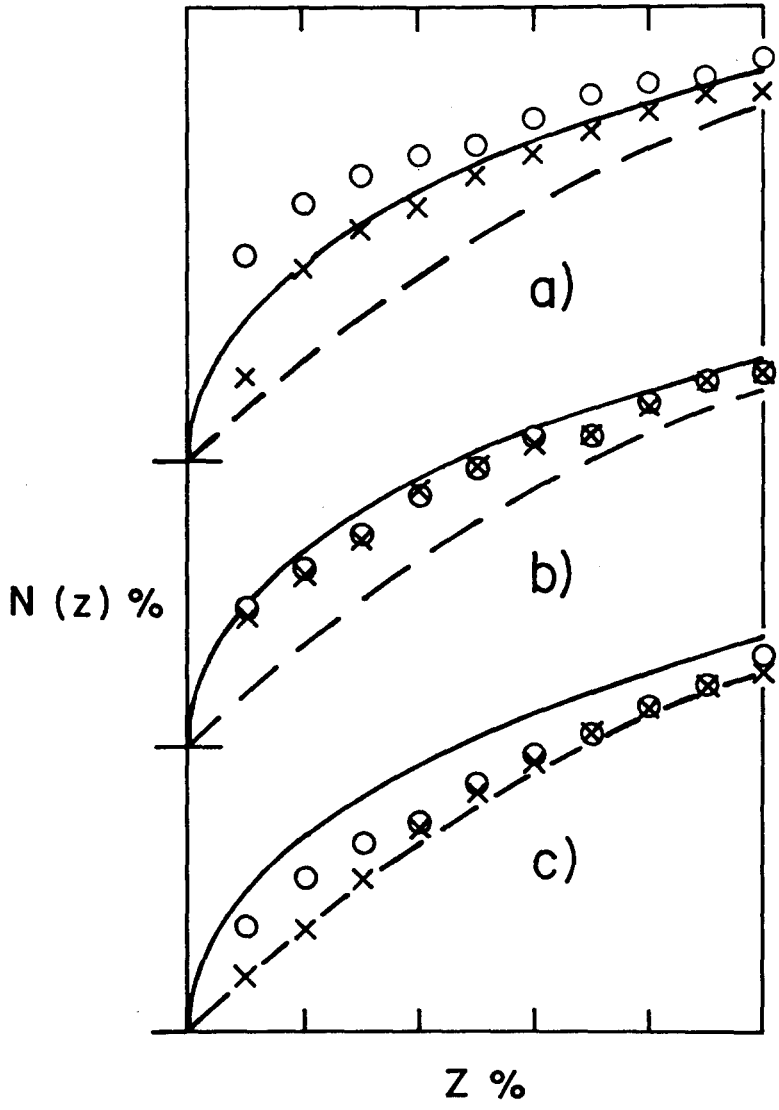


FIG. 9. $N(z)$ statistical test for center of symmetry. Solid line indicates theoretical intensity distribution for $\bar{1}$, dashed line that for 1. (a) Kammererite, modified from Brown and Bailey (1963). Upper array of circles using 109 observed $k = 3n$ reflections exhibits hypersymmetry. Lower array of crosses using 61 observed $k \neq 3n$ reflections is close to centrosymmetric locus. (b) Phlogopite—1M. Circles represent intensity distribution for 121 $k \neq 3n$ reflections calculated from centrosymmetric model, space group $C2/m$. Crosses represent calculated distribution for the same model distorted to space group $C2$ by tetrahedral cation ordering and concomitant adjustment of tetrahedral sizes. (c) Vermiculite, modified from Shirozu and Bailey (1966). Crosses represent intensity distribution for 256 observed $k \neq 3n$ reflections, circles that for 187 $k \neq 3n$ reflections calculated from centrosymmetric model (C2/c) resulting from refinement.

https://doi.org/10.1346/CCMN.1966.0140101 Published online by Cambridge University Press

the only examples of tetrahedral ordering so far found in layer silicates are in especially hydrous species—two chlorites and a vermiculite.

The recent refinement of a 2-layer vermiculite structure by Shirozu and Bailey (1966) illustrates especially well the problem of tetrahedral ordering and its genesis. It was determined from the mean T—O bond lengths and temperature factors that the composition of tetrahedron T_1 is $Si_{0.65}Al_{0.35}$ and of T_2 is $Si_{0.86}Al_{0.14}$. Because of the use of 822 observed three-dimensional reflections in repeated refinement cycles the observed difference in mean T—O bond lengths can be shown to be statistically significant. It was also determined that the exchangeable cation $Mg_{0.41}{}^{2+}$ is located vertically between the superposed T_1 positions in the talc tetrahedral sheets above and below. This gives local charge balance such that the positive charge of the exchangeable Mg^{2+} is linked directly to and is balanced by the excess negative charge on the T_1 tetrahedra due to the ordered substitution of Al for Si.

This vermiculite, from Llano, Texas, has formed by surface weathering of phlogopite-1M. Just a few inches below the surface the phlogopite is fresh and unaltered. The 2-layer sequence observed in the vermiculite is closer to the sequence found in the 1M structure than to any other mica structure because of the presence in both of *L* type shifts within the talc sheets. The vermiculite sequence can be derived from that of the 1M mica by linear $b/3$ displacements without rotation. This is a structurally sound transformation that suggests that the relative orientations of the layers within a vermiculite polytype may be controlled by the structure of the micaceous or chloritic parent material. But we have the paradox that tetrahedral ordering is not permitted in the ideal space group ($C2/m$) of the parent 1M mica, but is observed in the alteration product. It is difficult to believe that sufficient energy would be available during surface weathering to order an original disordered Si, Al distribution.

For ideal ease of conversion the parent 1M mica should be ordered in the particular 2-layer pattern observed for the vermiculite. This would require that the Si and Al atoms form a 2-layer superstructure of symmetry $C2/c$ within a framework that is otherwise 1-layer and of symmetry $C2/m$. Intensity calculations using layers distorted by ordering and tetrahedral rotation as in vermiculite but shifted into a mica sequence, indicate that the diagnostic $l = 2n + 1$ reflections would be extremely weak. The reflections could not be observed in the Llano parent mica in exposures up to 50 hours. Nor could any other deviation from $C2/m$ symmetry be observed.

Although this particular problem is not solved, it illustrates the contribution that crystallography can make to the elucidation of the genesis and mode of transformation of certain clay minerals. It also illustrates a need for a better understanding of the order–disorder process in clays.

POLYTYPE STABILITIES

Considerable attention has been paid in recent years to the different stacking sequences of layers that are theoretically possible within each clay

https://doi.org/10.1346/CCMN.1966.0140101 Published online by Cambridge University Press

mineral group and to observing which polytypes are actually formed in nature. Of special interest to clay mineralogists are the observed relative abundances of polytypes and any relationship that may exist between a polytype and its natural environment or its conditions of crystallization.

The corrugation of the basal oxygen surface has been cited often as being responsible for the prevalence of regular stacking sequences in dioctahedral species. It is equally likely that the morphology of the surface has considerable influence on *which* regular sequence forms. A second important factor is the location of the vacant octahedral site. It can be no accident that 2-layer sequences are infrequent in trioctahedral species but are especially common in dioctahedral species, as in dickite, nacrite, pyrophyllite, cookeite, and the $2M_1$ micas—muscovite, paragonite, and margarite. Because the layer sequences in these dioctahedral structures are not necessarily 2-layer *per se*, the common structural feature is the regular alternation of occupied and vacant sites along the Z axis. This type of alternation must be especially stable. By contrast, trioctahedral layers have relatively planar oxygen surfaces. This lack of structural control has been cited as the reason for the frequency of 1-layer structures and of irregular or random sequences in trioctahedral clays.

Newnham (1961) showed for the kaolins that six 1-layer and 108 2-layer dioctahedral structures are theoretically possible. He justified nature's preference for kaolinite as the only 1-layer form and dickite and nacrite as the only 2-layer forms on the basis of three structural features.

(1) The highly charged Si and Al cations tend to avoid superposition.

(2) The basal oxygens rotate toward the hydroxyls in the adjacent layer to strengthen the interlayer bond.

(3) The corrugation of the basal oxygen surface should fit into a corresponding corrugation in the hydroxyl surface.

The dickite and nacrite structures are the only 2-layer forms that satisfy all three criteria and are considered by Newnham to be the most stable configurations. The kaolinite structure does not satisfy the corrugation criterion but is the only 1-layer form to satisfy both of the other two criteria. Radoslovich (1963) has extended Newnham's analysis by pointing out that the O—H bond extending out from each OH should be nearly coplanar with the nearest two Al—OH bonds in the octahedral sheet. The favored interlayer sequences that minimize the angular strain in the O—H bond are those of kaolinite, dickite, and nacrite. The dickite structure is judged to be more stable than that of nacrite, in accord with its greater observed abundance.

Trioctahedral 7 Å structures have been shown by Nelson and Roy (1958) to crystallize in synthetic systems at lower temperatures than true 14 Å chlorites of similar composition. They favor the interpretation that the 7 Å structures are high energy forms that tend to crystallize early but are metastable. They may persist metastably for long periods or invert to chlorite.

Bailey and Brown (1962) have shown that there are four possible 14 Å chlorite layer types, arbitrarily designated I*a*, I*b*, II*a*, and II*b*. Theoretically,

https://doi.org/10.1346/CCMN.1966.0140101 Published online by Cambridge University Press

layers of the same type may be superimposed to form six semirandom stacking systems, twelve regular 1-layer structures, or an unknown, but very large, number of multiple-layer structures. In practice, the semirandom sequences are the most abundant. Shirozu and Bailey (1965) have correlated the observed abundances of the different layer types with the varying amounts of attraction and repulsion between the ions in the structures that result from different sequences of talc–brucite–talc sheets (Fig. 7). They considered three types of atomic interaction over distances up to 7 Å.

(1) Repulsion between brucite and talc sheet cations.

(2) Attraction between talc octahedral cations and brucite hydroxyls.

(3) Differences in the amount of attraction between talc surface oxygens and talc and brucite octahedral cations resulting from the direction of tetrahedral twist.

Shirozu and Bailey conclude that the II*b* layer type is the stable structure and that the I*b*, I*a*, and II*a* layer types are increasingly less favorable arrangements. The I*a* structure becomes the stable structure if there are very few interlayer cations and these are positioned according to local charge balance considerations, as in vermiculite. Bailey and Brown (1962) observed that there is a tendency for the less favorable I*b* and I*a* chlorite layer types to form metastably in low energy, diagenetic environments, inverting to the stable II*b* type during metamorphism. This suggests that most II*b* chlorite found in sediments will be of detrital origin, although growth of the stable form under diagnetic conditions cannot be precluded entirely.

Smith and Yoder (1956) have shown for micas that there are six simple stacking sequences plus a large number of more complex sequences that are theoretically possible. Because of the ditrigonal basal surfaces that result from tetrahedral rotation, Radoslovich (1959) has proposed that micas in which successive layers are related to one another by rotations of 0° or $\pm$ 120° should occur more frequently than those related by rotations of 180° or $\pm$ 60°. For the simple mica polytypes this means that the 1M, $2M_1$, and 3T structures should be more abundant than the $2M_2$, 2O, and 6H structures, in accord with observation.

Yoder and Eugster (1955) showed in synthetic systems that the growth sequence for muscovite of $1Md \rightarrow 1M \rightarrow 2M_1$ is favored by longer duration runs or by higher temperatures. Velde (1965) has shown that $2M_1$ is the stable structure for the ideal muscovite composition and that both 1Md and 1M are metastable. He suggests that the occurrence of the latter polytypes in sedimentary, low-grade metamorphic, and hydrothermal environments is a result either of early crystallization of metastable products according to Ostwald's step rule or of enhancement of their stability by compositional variation. Several studies have demonstrated that the $2M_1$ muscovite present in sediments is probably of detrital origin. This has been confirmed by K–Ar dating for a few samples in which it proved possible to separate the $2M_1$ and mixed layer clay components (Bailey *et al.*, 1962).

The writer's interpretation of the consensus of recent studies on the nature

https://doi.org/10.1346/CCMN.1966.0140101 Published online by Cambridge University Press

of sedimentary *illite* is that it is a heterogeneous mixture of detrital $2M_1$ muscovite, detrital mixed layer micaceous weathering products, detrital weathering products partly reconstituted by K-adsorption or by diagenetic growth of chloritic interlayers, plus true authigenic 1Md and 1M micas—some having mixed layering also. The proportions of these components may vary widely depending on a complex interaction of variables, including location of the sedimentary basin relative to source areas, the composition, relief, and climate of the source areas, chemical composition of the basin and of later interstratal waters, depth of burial, and geologic age.

In summary, the stable clay mineral polytypes are the most abundant. Judging by the examples of muscovite—$2M_1$ and chlorite (II*b*), the stable polytype occurs nearly to the exclusion of other polytypes in environments where sufficient thermal energy or pressure are available. This includes medium- to high-grade metamorphic rocks, igneous rocks, most pegmatites, and most medium to high temperature ore deposits. Metastable polytypes crystallize early and may persist indefinitely at low temperatures. These polytypes are the ones most apt to form diagenetically in sediments, by alteration and replacement by low temperature solutions, or by low-grade metamorphism.

If the interpretation above is correct, the success of the clay mineralogist in using clay minerals as indicators of geologic environments will depend on a knowledge as to which polytypes are metastable, which are the most reliable indicators of low temperature occurrence (perhaps because of being the most resistant to conversion to the stable form), and the variations in stability that are possible as a result of compositional variation. The higher temperature, stable polytypes can usually be judged of detrital origin when found in sediments or soils. But this does not preclude partial reconstitution of a degraded stable polytype in the sedimentary environment or even the authigenic growth of the stable form under the right conditions. An analogy can be made with authigenic feldspars. The common authigenic K-feldspar is a monoclinic, metastable form, but occasionally the triclinic, fully ordered microcline crystallizes.

REFERENCES

BAILEY, S. W., and BROWN, B. E. (1962) Chlorite polytypism: I. Regular and semi-random one-layer structures: *Amer. Min.* **47**, 819–50.

BAILEY, S. W., HURLEY, P. M., FAIRBAIRN, H. W., and PINSON, W. H. (1962) K–Ar dating of sedimentary illite polytypes: *Geol. Soc. Amer. Bull.* **73**, 1167–70.

BROWN, B. E., and BAILEY, S. W. (1963) Chlorite polytypism: II. Crystal structure of a one-layer Cr-chlorite: *Amer. Min.* **48**, 42–61.

BURNHAM, CHARLES W., and RADOSLOVICH, E. W. (1965) Refinement of the crystal structures of coexisting muscovite and paragonite: *Clays and Clay Minerals*, Proc. 13th Conf., Pergamon Press, New York (in press).

BURNS, ALLAN F., and WHITE, JOE L. (1963) The effect of potassium removal on the *b*-dimension of muscovite and dioctahedral soil micas: *Proc. Internat. Clay Conf., Stockholm*, Pergamon Press, New York, pp. 9–16.

https://doi.org/10.1346/CCMN.1966.0140101 Published online by Cambridge University Press

DONNAY, GABRIELLE, DONNAY, J. D. H., and TAKEDA, HIROSHI (1964) Trioctahedral one-layer micas. II. Prediction of the structure from composition and cell dimensions: *Acta Cryst.* **17**, 1374–81.

EGGLETON, R. A., and BAILEY, S. W. (1966) Structural aspects of dioctahedral chlorite: *Amer. Min.* **51** (in press).

LINDQVIST, BENGT (1962) Polymorphic phase changes during heating of dioctahedral layer silicates: *Geol. Foren. Forhandl.* **84**, 224–9.

NELSON, BRUCE W., and ROY, RUSTUM (1958) Synthesis of the chlorites and their structural and chemical constitution: *Amer. Min.* **43**, 707–25.

NEWNHAM, ROBERT E. (1961) A refinement of the dickite structure and some remarks on polymorphism in kaolin minerals: *Min. Mag.* **32**, 683–704.

RADOSLOVICH, E. W. (1959) Structural control of polymorphism in micas: *Nature* **183**, 253.

RADOSLOVICH, E. W. (1963) The cell dimensions and symmetry of layer-lattice silicates. IV. Interatomic forces: *Amer. Min.* **48**, 76–99.

SHIROZU, HARUO, and BAILEY, S. W. (1965) Chlorite polytypism: III. Crystal structure of an orthohexagonal iron chlorite: *Amer. Min.* **50**, 868–85.

SHIROZU, HARUO, and BAILEY, S. W. (1966) Crystal structure of a two-layer Mg-vermiculite: *Amer. Min.* **51** (in press).

SMITH, J. V., and BAILEY, S. W. (1963) Second review of Al—O and Si—O tetrahedral distances: *Acta Cryst.* **16**, 801–11.

SMITH, J. V., and YODER, H. S. (1956) Experimental and theoretical studies of the mica polymorphs: *Min. Mag.* **31**, 209–35.

STEINFINK, HUGO (1958) The crystal structure of chlorite. I. A monoclinic polymorph: *Acta Cryst.* **11**, 191–5.

STEINFINK, HUGO (1961) Accuracy in structure analysis of layer silicates: Some further comments on the structure of prochlorite: *Acta Cryst.* **14**, 198–9.

TAKÉUCHI, Y. (1965) Structures of brittle micas: *Clays and Clay Minerals*, Proc. 13th Conf., Pergamon Press, New York (in press).

THREADGOLD, I. M. (1963) The crystal structures of hellyerite and nacrite: Ph.D. thesis, Univ. Wisconsin.

VEITCH, L. G., and RADOSLOVICH, E. W. (1963) The cell dimensions and symmetry of layer-lattice silicates. III. Octahedral ordering: *Amer. Min.* **48**, 62–75.

VELDE, B. (1965) Experimental determination of muscovite polymorph stabilities: *Amer. Min.* **50**, 436–49.

YODER, H. S., and EUGSTER, H. P. (1955) Synthetic and natural muscovites: *Geochim. Cosmochim. Acta* **7**, 225–80.

https://doi.org/10.1346/CCMN.1966.0140101 Published online by Cambridge University Press